Formation of Replicating Saponite from a Gel in the Presence of Oxalate: Implications for the Formation of Clay Minerals in Carbonaceous Chondrites and the Origin of Life

ASTROBIOLOGY
Volume 12, Number 6, 2012

DOI: 10.1089/ast.2011.0635

Formation of Replicating Saponite from a Gel in the Presence of Oxalate: Implications for the Formation of Clay Minerals in Carbonaceous Chondrites and the Origin of Life

Dirk Schumann,[1] Hyman Hartman,[2] Dennis D. Eberl,[3] S. Kelly Sears,[4] Reinhard Hesse,[1] and Hojatollah Vali[1,4]

Abstract

The potential role of clay minerals in the abiotic origin of life has been the subject of ongoing debate for the past several decades. At issue are the clay minerals found in a class of meteorites known as carbonaceous chondrites. These clay minerals are the product of aqueous alteration of anhydrous mineral phases, such as olivine and orthopyroxene, that are often present in the chondrules. Moreover, there is a strong correlation in the occurrence of clay minerals and the presence of polar organic molecules. It has been shown in laboratory experiments at low temperature and ambient pressure that polar organic molecules, such as the oxalate found in meteorites, can catalyze the crystallization of clay minerals. In this study, we show that oxalate is a robust catalyst in the crystallization of saponite, an Al- and Mg-rich, trioctahedral 2:1 layer silicate, from a silicate gel at 60°C and ambient pressure. High-resolution transmission electron microscopy analysis of the saponite treated with octadecylammonium ($n_C = 18$) cations revealed the presence of 2:1 layer structures that have variable interlayer charge. The crystallization of these differently charged 2:1 layer silicates most likely occurred independently. The fact that 2:1 layer silicates with variable charge formed in the same gel has implications for our understanding of the origin of life, as these 2:1 clay minerals most likely replicate by a mechanism of template-catalyzed polymerization and transmit the charge distribution from layer to layer. If polar organic molecules like oxalate can catalyze the formation of clay-mineral crystals, which in turn promote clay microenvironments and provide abundant adsorption sites for other organic molecules present in solution, the interaction among these adsorbed molecules could lead to the polymerization of more complex organic molecules like RNA from nucleotides on early Earth. Key Words: Saponite—2:1 layer silicates—Origin of life—Silicate-organics interactions—Oxalate as a catalyst—Crystallization of saponite from silica gel. Astrobiology 12, 549–561.

1. Introduction

It has been proposed that the processes of abiotic synthesis of organic compounds that led to the first primitive life-forms occurred in the vicinity of hot springs on an outgassing early Earth (Shock, 1990; Delaney *et al.,* 1998; Cody *et al.,* 2004). The potential role of clay minerals in these processes was first recognized by Bernal (1949), who suggested that their surfaces are the likely location where organic molecules that occurred in warm tidal ponds or in the ocean (primordial "soup") could concentrate and polymerize more complex organic compounds such as amino acids. These ideas were further developed by Cairns-Smith (1965), Cairns-Smith and Hartman (1986), Balogh and Laszlo (1993), Ertem and Ferris (1996), Hanczyc *et al.* (2003), and Meunier *et al.* (2010).

Hartman *et al.* (1993) proposed, moreover, that the complex interaction between polar organic compounds and clay-mineral formation in carbonaceous chondrites, a class of meteorite, would be indicative of what may have occurred on early Earth. Carbonaceous chondrites are considered to be among the most primitive materials from the early stages of the Solar System. Owing to their almost unfractionated nature, carbonaceous chondrites are representative of the processes that occurred in solid objects in the early Solar System (Chang and Bunch, 1986). These meteorites contain varying amounts of anhydrous mineral phases, such as olivine, orthopyroxene, melilite, spinel, perovskite, and metal oxides,

[1]Department of Earth and Planetary Sciences, McGill University, Montréal, Québec, Canada.
[2]Department of Biomedical Engineering, Massachusetts Institute of Technology, Cambridge, Massachusetts, USA.
[3]United States Geological Survey, Boulder, Colorado, USA.
[4]Facility for Electron Microscopy Research, McGill University, Montréal, Québec, Canada.

as well as mixtures of hydrous alteration products, such as phyllosilicates (*e.g.,* saponite, serpentine), hydroxides, oxyhydroxides, and hydrous sulfides, all of which form the matrix of the chondrules (Bass, 1971; Bunch and Chang, 1980; Barber, 1981; Chang and Bunch, 1986; McSween, 1987; Brearley, 1997; Tomeoka and Ohnishi, 2010). The hydrous phases are the predominant minerals. The textural relationship of the hydrous alteration products to the remaining unaltered primary minerals (*e.g.,* olivine, orthopyroxene) suggests *in situ* aqueous alteration (Anders, 1963; Chang and Bunch, 1986; Brearley, 1997; Tomeoka and Ohnishi, 2010). Besides these minerals, carbonaceous chondrites also contain significant amounts of carbon bound into inorganic phases, particularly carbonates, and organic compounds, such as carboxylic acids, hydrocarbons, amino acids, ketones, aldehydes, alcohols, amines, and acid-insoluble polymers (Chang and Bunch, 1986).

A very strong positive correlation exists between the concentration of polar organic compounds and clay minerals (Becker and Epstein, 1982; Hartman *et al.,* 1993; Pizzarello *et al.,* 2003; Glavin and Dworkin, 2009). Pizzarello *et al.* (2003) reported the correlation between the amino acid isovaline and hydrous silicate abundance in some fragments from the Murchison meteorite. Glavin and Dworkin (2009) provided additional evidence that the formation of an excess of L–amino acid may have been the result of a secondary process that involves the aqueous interaction of lithic components. These authors investigated the distribution and enantiomeric composition of the five-carbon (C_5) amino acids found in CI-, CM-, and CR-type carbonaceous meteorites (CI, Ivuna group; CM, Mighei group; CR, Renazzo group). A large enrichment of the amino acid isovaline was found in the CM meteorite Murchison and the CI meteorite Orgueil. They concluded that the enrichment of isovaline in these two carbonaceous meteorites could not have been the result of interference from other C_5 amino acid isomers present in the samples, analytical bias, or terrestrial amino acid contamination. Since similar enrichments do not occur in most primitive unaltered carbonaceous chondrites (Antarctic CR meteorites EET 92042 and QUE 99177), it was concluded that the driving force behind L-isovaline enrichment was an extensive aqueous alteration phase on the parent bodies of the meteorites.

The aqueous alteration phase could have resulted from the melting of ice and outgassing of the planetoid parent body (Bunch and Chang, 1980; Jones *et al.,* 1990; Hartman *et al.,* 1993). Electromagnetic induction heating of meteorite parent bodies in a strong solar wind in the T Tauri phase of the Sun and radioactive decay within the planetoid have been discussed as potential heat sources needed for the formation of such aqueous phases (Lee, 1979; Jones *et al.,* 1990; Shimazu and Terasawa, 1995). The heating of a parental planetoid body through internal heat sources creates a zone in which liquid water can exist. The temperature of aqueous alteration has been estimated to have been in the range of 300 K (27°C) to <373 K (100°C) (Anders, 1963; Jones and Brearley, 2006).

Thus far, amino acids have received the most attention, but carboxylic acids (*e.g.,* oxalic acid) are found in much greater abundance in carbonaceous chondrites (Cronin *et al.,* 1993). For example, the presence of oxalic acid in the liquid water phase could have enhanced the alteration of olivine and pyroxene to form Mg- and Fe-rich phyllosilicates like serpentine or saponite (Hartman *et al.,* 1993). The clay minerals might have played an important role in the enrichment of chiral L–amino acids like isovaline ("left"-handed amino acids) in the carbonaceous chondrites as described by Glavin and Dworkin (2009). A chiral molecule, like isovaline, does not have an internal plane of symmetry and therefore cannot be superimposed on a mirror image. In biological systems, most compounds have the same chirality. For example, most amino acids are all "left"-handed, and most sugars are "right"-handed. The template-catalyzed polymerization of clay formation could be a possible amplification mechanism for the enrichment of chiral molecules in carbonaceous chondrite meteorites. In recent studies, Fraser *et al.* (2011a, 2011b) provided experimental evidence for the chiral enrichment of amino acids on vermiculite crystals. It is therefore important from the point of view of prebiotic chemistry whether organic acids like oxalic acid might have catalyzed the formation of the phyllosilicate phases on these meteorites. Hartman (1998) suggested that the formation of Fe- and Mg-rich smectite-group minerals, particularly saponite, could be catalyzed by polar organic molecules, such as oxalate and amino acids, in the warm lagoons and tidal ponds of early Earth. Saponite is an authigenic 2:1 clay mineral commonly formed by low-temperature (<100°C) and low-pressure (~1 bar) abiotic geochemical processes such as the alteration of oceanic crust and continental mafic rocks (Velde and Meunier, 2008). In some modern deep marine, shallow marine, and subaerial hydrothermal environments, however, the precipitation of saponite appears to be biologically induced (Drits *et al.,* 1989; Koehler *et al.,* 1994; Marteinsson *et al.,* 1997; Geptner *et al.,* 2002).

Siffert (1962) found that oxalic acid catalyzed the formation of clay minerals in the laboratory at ambient temperatures. Subsequent studies investigated the catalytic role of other organic acids, such as fulvic and humic acid, in the synthesis of the 1:1 layer silicate kaolinite (Linares and Huertas, 1971; La Iglesia and Martin Vivaldi, 1972; Hem and Lind, 1974; La Iglesia and Galan, 1975). Clay mineral synthesis is possible because of the complexing properties of the organic anions with aluminum, iron, or magnesium cations. The presence of organic aluminum complexes adjusts the SiO_2/Al_2O_3 ratio of the solution and prevents or slows down the polymerization of hydrolyzed metal cations into hydroxide species (Hem and Lind, 1974; Siffert, 1986). These organic complexes also favor the formation of phyllosilicates rather than the precipitation of a hydroxide gel (Siffert, 1986). Small *et al.* (1992) and Small and Manning (1993) showed that oxalate anions act as a catalyst to enhance 2:1 clay-mineral precipitation by destabilizing the gel and increasing Al solubility. Organic anions that form complexes with aluminum, magnesium, and ferrous cations not only increase their solubility but also adjust pH toward neutrality and thus enhance the formation of ionic species reacting with silica (Siffert, 1986). The dissolution of the gel also makes the other ions like Mg^{2+}, Si^{4+}, and K^+ available for the crystallization reactions. It is also useful to remember that oxalate is most effective as a catalyst at low temperature and pressure, and it is these temperatures and pressures that are most relevant to prebiotic chemistry.

The objectives of this study, therefore, were to (i) demonstrate the catalytic effect of oxalic acid on the nucleation and growth of saponite from a silicate gel at 60°C and 1

atmospheric pressure, (ii) characterize the composition and structure of the 2:1 silicate layers that comprise the synthetic saponite, and (iii) evaluate the replicating capability of saponite.

2. Materials and Methods

2.1. Synthesis of saponite

The saponite investigated in this study was synthesized from a silicate gel produced by Whitney (1983) following the method outlined by Hamilton and Henderson (1968). The structural formula of saponite differs from other smectite-group minerals in that it has a positive charge emanating from the octahedral sheet that compensates partially for the negative charge from the tetrahedral sheet. The following structural formula for saponite

$$R^{n+}_{(x-y)/n}mH_2O(Mg_{3-y}R^{3+}_y)(OH)_2(Si_{4-x}Al_x)O_{10}$$

from Brindley (1981) takes this potential positive octahedral charge into consideration, with R^{3+} mostly represented by Fe^{3+}, while the interlayer space R^{n+} can be filled by Na^+, K^+, Ca^{2+}, and mH_2O. However, if no Fe^{3+} is available in the system, the octahedral sheet may only contain Mg^{2+}, and no positive charge arises from the octahedral sheet.

The chemical composition of the silicate gel used in this study expressed in weight percent oxide consists of 56.25% SiO_2, 4.30% Al_2O_3, 30.88% MgO, and 3.97% K_2O. The cation ratios of that gel would correspond to the following formula for saponite

$$K_{0.33}Mg_3(OH)_2(Si_{3.67}Al_{0.33})O_{10}$$

Two sets of synthesis experiments were conducted with both sets containing 315 mg silicate gel powder; however, in experiment 1, 30 mL of 0.5 *M* solution of disodium oxalate ($Na_2C_2O_4$) was admixed, while 30 mL of 3 *N* NaOH solution was added to experiment 2. The samples were transferred into tightly sealed centrifuge tubes (Oak Ridge style) and placed on an end-over-end mixer to assure constant agitation in an oven at 60°C and atmospheric pressure.

2.2. X-ray diffraction and transmission electron microscopy analysis

The synthesis products were extracted after 3 months and prepared for investigation by X-ray diffraction (XRD) and transmission electron microscopy (TEM). For the XRD analysis, oriented air-dried samples were prepared by dispersing ~50 mg of material in distilled water, transferring the suspension onto glass slides, and drying at room temperature for 24 h. After X-raying, the air-dried samples were solvated with ethylene glycol (EG) under vapor pressure at 60°C for 24 h and immediately re-analyzed by XRD. Owing to insufficient amounts of sample material produced in the presence of NaOH (experiment 2), an *n*-alkylammonium-treated XRD sample was only prepared from the synthesis product that crystallized in the presence of oxalate (experiment 1). For this treatment method, approximately 40 mg of dried material was placed in a 1.5 mL polypropylene Eppendorf micro test tube and dehydrated with 100% ethanol for 24 h. After centrifugation, the ethanol was removed, and the sample was dispersed in a 0.05 *N* solution of octadecylamine hydrochloride and left in an oven at 65°C for 24 h. This exchange procedure was repeated five times. The sample was washed up to 15 times with 100% ethanol to remove excess octadecylammonium ($n_C = 18$) salts. The washed clay material was dispersed in ~1 mL of 100% ethanol and pipetted onto a glass slide, dried at room temperature, and X-rayed. XRD analyses of the air-dried and EG-solvated samples were performed on a Siemens D500 diffraction system, while the X-ray analysis of the $n_C = 18$ treated sample was conducted with a Rigaku D/MAX 2400 12kW rotating anode diffractometer. In both cases, Cu-Kα radiation, a 0.02 degree step size, and a counting time of 2 s per step were used. Both systems are equipped with a graphite monochromator.

For the TEM investigation of particle shape, small amounts of the synthesis products from experiments 1 and 2 were dispersed in distilled water and transferred onto 300-mesh Cu TEM grids with carbon support film. For high-resolution transmission electron microscopy (HRTEM) investigation, the synthesis products of experiment 1 were embedded with Epon resin. Approximately 10–20 mg of the clay material was placed in 1.5 mL polypropylene Eppendorf micro test tubes and dehydrated by adding 100% acetone to remove adsorbed water. After centrifugation at 13,000 rpm for 15 min, the supernatant was removed and the clay material dispersed in a mixture of 10% Epon resin and 90% acetone by ultrasonic treatment. These steps were repeated with mixtures containing 30%, 50%, 70%, and 100% resin. To obtain a full dispersion of the material, the acetone-resin mixtures were agitated in an ultrasonic bath for ~60 s.

Each incubation step lasted 24 h with the samples placed onto a rotator to ensure continuous agitation. The resin-clay mineral mixture was transferred into embedding moulds after the fifth incubation step (100% Epon resin). After a settling time of 1–2 h, the embedding moulds were transferred into an oven at 65°C for 48 h. Ultrathin sections (70–80 nm) were cut from the polymerized resin blocks with an ultramicrotome and transferred onto 300-mesh Cu TEM grids with carbon support film.

Octadecylammonium cation ($n_C = 18$) exchange was carried out by using a modified version of the procedure described by Vali and Hesse (1990). Each grid was placed face down into a 1.5 mL micro test tube on the surface of 0.5 *M* solution of octadecylamine hydrochloride diluted to 50% at 65°C and placed into the oven for 20 min. The grids were removed from the tubes, submerged into a Petri dish filled with distilled water preheated to 65°C, and gently agitated for several minutes to remove excess $n_C = 18$ cations or octadecylammonium salts. The samples were characterized with a Philips CM200 TEM equipped with an AMT XR41B CCD camera system and an EDAX Genesis energy-dispersive X-ray spectroscopy system in bright-field mode at an accelerating voltage of 200 kV. Lattice fringe images were taken at Scherzer defocus (underfocus) conditions (Vali *et al.*, 1991; Vali and Hesse, 1992).

2.3. n-Alkylammonium cation-exchange method

The *n*-alkylammonium cation-exchange method was developed by Lagaly and Weiss (1969) as a tool to determine the interlayer charge density, layer charge, and charge distribution of expandable 2:1 layer silicates, such as smectite-group

minerals, vermiculitic minerals, and illitic minerals in XRD. For long-chain *n*-alkylammonium cations such as $n_C = 18$, the arrangement of the *n*-alkylammonium cations within the 2:1 layer silicate interlayers depends upon the magnitude of the layer charge and the charge density. Low-charge smectite-group minerals will have flat-lying monolayer (~13.6 Å), bilayer (~17.7 Å), or pseudotrimolecular (21.7 Å) arrangements, while higher-charge smectite-group minerals, vermiculite-group minerals, expandable illite, or altered micas show paraffin-type arrangements of the *n*-alkylammonium cations (25 to >30 Å) (Fig. 1). For a detailed summary of the theoretical background of the *n*-alkylammonium cation-exchange method and additional references see the work of Sears *et al.* (1998).

3. Results

3.1. Experiment 1: silicate gel + disodium oxalate ($Na_2C_2O_4$)

The XRD pattern of the air-dried starting silicate gel reveals its amorphous nature (Fig. 2a). A very small broad peak, however, suggests the presence of a minor amount of Al_2O_3 that was not incorporated into the gel structure. XRD patterns of air-dried synthesis products obtained after 3 months show a low-angle shoulder between 5 and 8° 2θ, which corresponds to a first-order reflection (S_{001}) of saponite (Fig. 2b). Upon EG solvation, the first-order reflection S_{001} shifted towards a lower 2θ angle (5° or d = 17.52 Å) and was significantly more pronounced than in the air-dried pattern (Fig. 2c). Two sharp reflections that appear around 9.19–9.22 Å and 3.09 Å most likely represent the (001) and (003) basal reflections of talc (T_{001}, T_{003}), a by-product of the synthesis (Fig. 2b, 2c). The talc T_{001} and T_{003} reflections did not change their positions after EG solvation. The diffraction pattern of the sample treated with $n_C = 18$ shows a first-order reflection around 5° 2θ (17.76 Å) (Fig. 2d). In general, the weak intensities of the peaks are due to the limited amount of sample material available for $n_C = 18$ treatment. The weak peaks around 20° 2θ in the air-dried, EG-solvated, and $n_C = 18$ treated sample are most likely the hk reflections of saponite, which are seen because the clay is not perfectly oriented (Fig. 2b–d).

TEM investigation of the synthesis products obtained after 3 months at low magnification showed clusters of globular aggregates that consist of packets of saponite crystals (Fig. 3a, 3b). The saponite crystals have a whisker-like appearance within these globules. Lattice-fringe images of the ultrathin sections treated with $n_C = 18$ cations enabled the analysis of the internal structure of the globules (Fig. 3c, 3d). The packets of saponite 2:1 silicate layers within these whiskers are tapered toward the outside (Fig. 3c, 3d).

Lattice-fringe images of the 3-month synthesis product after treatment with $n_C = 18$ cations show the presence of (1) single double layers and short sequences of three to eight 2:1 silicate layers that have expanded interlayers of ~13.6 Å (white half circles in Fig. 4a, 4b), (2) sequences of two to 10

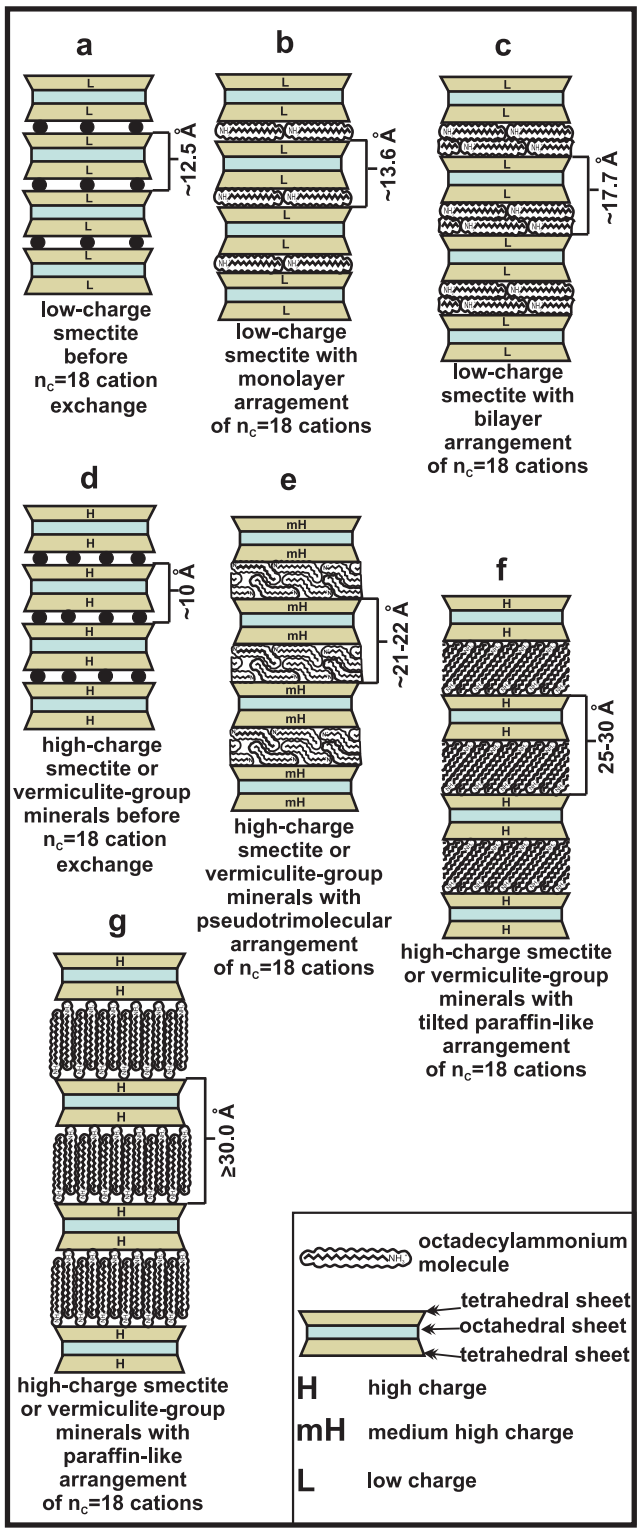

FIG. 1. Model showing smectite-group or vermiculite-group 2:1 layer silicates before and after treatment with octadecylammonium ($n_C = 18$) cations (not to scale): (**a**) low-charge smectite-group mineral, (**b**–**c**) low-charge smectite-group mineral with a monolayer (13.6 Å) and bilayer (17.7 Å) arrangement of the $n_C = 18$ cations, (**d**) high-charge smectite-group or vermiculite-group 2:1 layer silicates, (**e**) high-charge smectite-group or vermiculite-group 2:1 layer silicates with a pseudotrimolecular (21–22 Å) arrangement of $n_C = 18$ cations, (**f**–**g**) paraffin-like arrangement of $n_C = 18$ cations with different tilt angles of the alkyl chains. Compilation based on the original drawings of Lagaly and Weiss (1969, 1970), Lagaly (1981), and Vali *et al.* (1994). Color images available online at www.liebertonline.com/ast

curved to planar 2:1 silicate layers that have expanded interlayer spacing ranging from ~25 to ~33 Å (white diamonds in Fig. 4b–d), (3) minor amounts of packets of 2:1 silicate layers that consist of both 13.6 Å layers and 25–33 Å layers (Fig. 4d), and (4) clusters of disorganized single 2:1 silicate layers (white circle in Fig. 4e).

Energy-dispersive spectroscopy (EDS) analyses of the samples treated with $n_C = 18$ cations revealed the predominance of Si and Mg over Al in the 2:1 silicate layers of the saponite crystallites (Fig. 5). The EDS spectra did not show any K^+ or Na^+ since the interlayer cations were exchanged with the $n_C = 18$ cations, which resulted in the interlayer expansion of the sequences. The 13.6 Å spacing observed suggests monolayer arrangements of the $n_C = 18$ cations characteristic for an average interlayer charge of < 0.4 eq/$O_{10}(OH)_2$ for low-charge smectite-group minerals. The sequences with the expansion ranging from 25 to 33 Å have a paraffin-like intercalation of the $n_C = 18$ molecules (Figs. 1, 4, 5) (Lagaly and Weiss, 1969, 1970; Lagaly, 1981, 1982). This arrangement of $n_C = 18$ molecules may occur in 2:1 layer silicates that have interlayer charges as low as 0.63 eq/$O_{10}(OH)_2$ (Lagaly, 1982; Malla and Douglas, 1987; Lagaly and Dékany, 2005).

3.2. Experiment 2: silicate gel + sodium hydroxide (NaOH)

In contrast to the material from experiment 1, the XRD patterns of the air-dried synthesis products do not show a first-order reflection between 5° and 8° 2θ as expected for saponite (Fig. 2e). After EG solvation, however, a weak hump is observable between 5 and 8° 2θ, the region where one would expect the first-order reflection of a smectite-group mineral like saponite (Fig. 2f). A talc-like phase also crystallized during this experiment as evident by the presence of 9.13 and 3.10 Å reflections. The peak present at 7.75 Å may be interpreted as a first-order reflection of a very poorly crystallized serpentine with a second-order reflection at 3.83 Å. The peaks at 4.71 and 2.34 Å may be associated with a brucite-like phase.

Low-magnification TEM images show the presence of globular aggregates of randomly oriented whisker-like and needle-like crystals as well as aggregates of tabular particles (Fig. 6a, 6b). EDS analyses showed Mg, Si, and Al as the dominant elements in the lumps of whisker- and needle-shaped particles, but only Mg in the tabular crystals (Fig. 6c, 6d). The larger whisker-like bundles most probably correspond to the saponite phase (Sap), while the fine needle-like aggregates could be associated with the poorly crystallized serpentine phase (Ser) as indicated by XRD (Fig. 6e). Since both phases would contain Mg and Si, a mixture of these two phases would not be distinguishable by EDS. The tabular crystals seem to be brucite (Bru). The majority of these crystals have an anhedral crystal habit (black arrows in Fig.

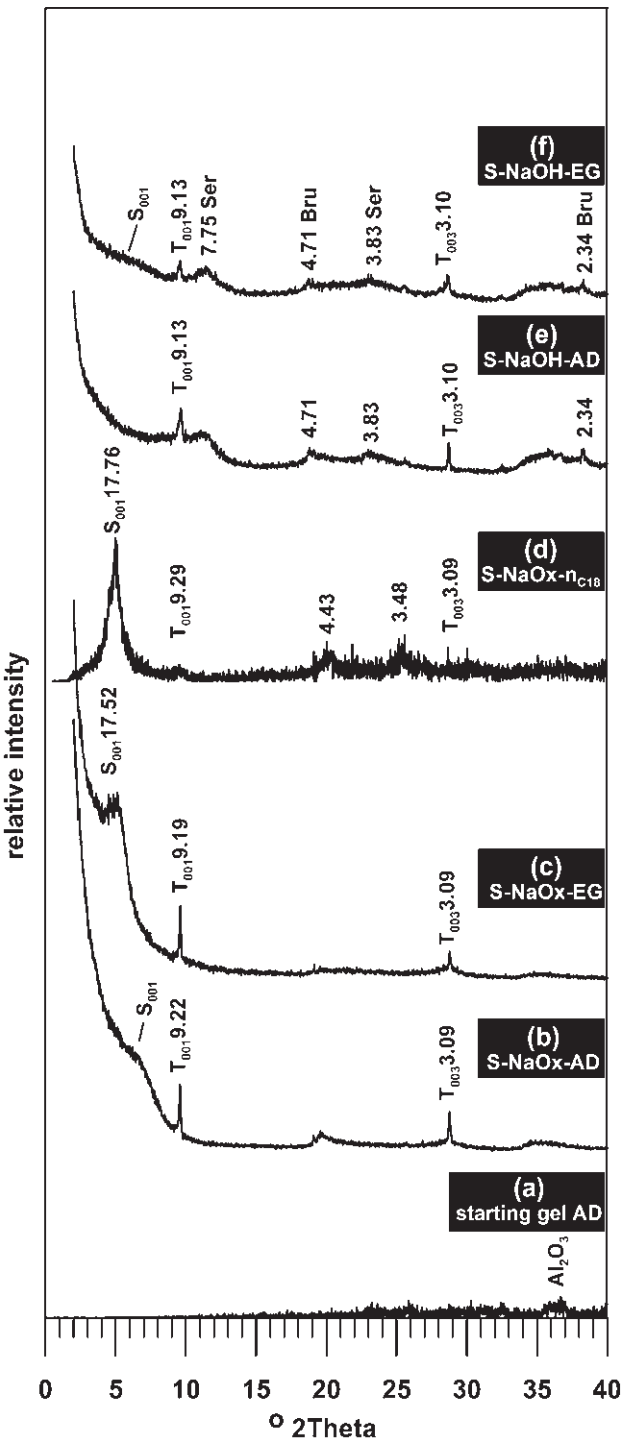

FIG. 2. XRD patterns of the products of saponite synthesis experiments 1 and 2. (**a**) Air-dried (AD) starting silica gel; (**b–c**) air-dried and ethylene glycol–solvated (EG) synthesis products of experiment 1 extracted after 3 months; (**d**) 3-month synthesis product of experiment 1 treated with $n_C = 18$ cations. The XRD patterns for experiment 1 show the presence of saponite (S) and a talc-like phase (T) as synthesis products. (**e–f**) Air-dried and ethylene glycol–solvated (EG) synthesis products of experiment 2 also extracted after 3 months. The XRD patterns for experiment 2 show the presence of saponite (S), a talc-like phase (T), brucite (Bru), and a poorly crystallized serpentine-like mineral phase (Ser). Subscript numbers indicate basal reflections of the identified phases [S_{001} = (001) reflection of saponite, T_{001} = (001) reflection of talc]. Numbers describe the spacing in ångströms (Å). NaOx, disodium oxalate solution; $n_C = 18$, octadecylammonium cations; NaOH, sodium hydroxide solution.

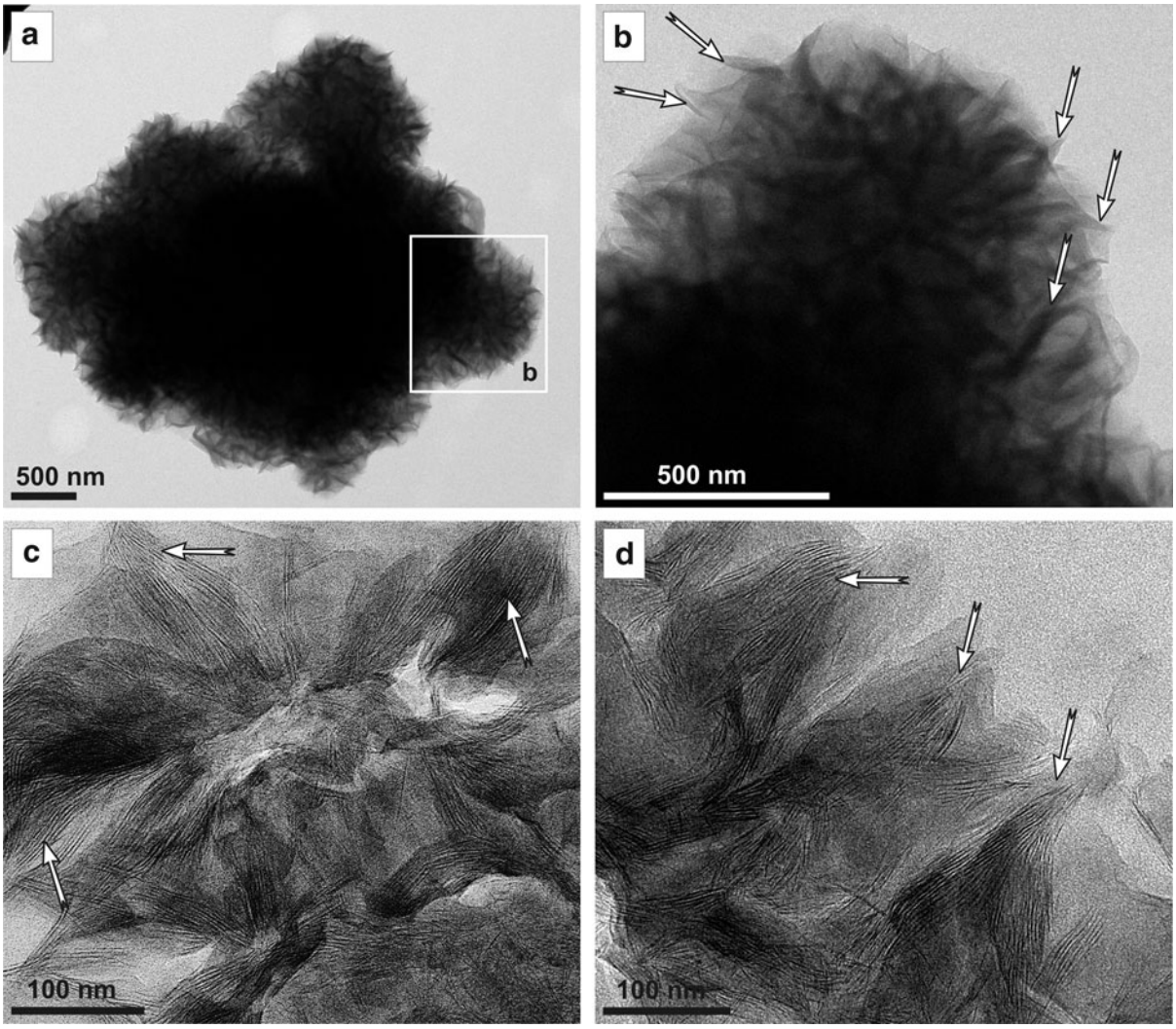

FIG. 3. TEM images of the synthesis products of experiment 1. (**a**–**b**) Overview images showing globular aggregates of synthesized saponite crystals. The saponite crystals have a whisker-like appearance in these globules (white arrows in b); (**c**–**d**) HRTEM images of the whisker-like saponite crystal packets as seen in (b) (white arrows).

6e, 6f). In some cases, however, well-developed crystal faces are visible (white arrows in Fig. 6b). Small aggregates of saponite crystals on top of brucite crystals may suggest that the latter could act as nucleation sites for saponite (white diamonds in Fig. 6b, 6f). It could, however, also be an artifact of sample preparation. The saponite aggregates have a much less developed globular shape in this experiment compared to experiment 1 (compare Figs. 3a, 3b, and 6a).

4. Discussion

The catalyzing effect of oxalate on the formation of saponite can clearly be seen in the EG-solvated XRD patterns and the TEM images of experiments 1 and 2 (compare Figs. 2c and 2f). The experimental run with the disodium oxalate solution shows a more pronounced first-order saponite reflection than the run with the NaOH solution. Low-magnification TEM images of the synthesis products of experiment 1 (oxalate) show well-defined, globule-like aggregates of packets of saponite. The aggregates of saponite and possibly serpentine in experiment 2 do not have an equally well-developed globular shape. It is clear that under the given experimental conditions oxalate is a better catalyzing agent than NaOH for the crystallization of saponite. The formation of saponite from a silica gel at 60°C and 1 atmospheric pressure in the presence of oxalate may mimic the conditions of surface temperature and pressure during the early Archean (Zahnle *et al.*, 2007) as well as the near-surface conditions of planetoid parent bodies, such as carbonaceous chondrites (Glavin and Dworkin, 2009), that formed during the early stages of the Solar System (see Introduction).

The XRD data of the synthesis products of experiment 1 treated with $n_C = 18$ cations show saponite as the dominant phase with a first-order reflection of 17.67 Å. This spacing would suggest a bilayer arrangement of the $n_C = 18$ cations in the interlayer space. There is, however, a discrepancy between XRD data and the observations made in the HRTEM images. Lattice-fringe images of the synthesized 2:1 layer silicates exchanged with $n_C = 18$ cations show a different expansion behavior. Two phases can be recognized: a

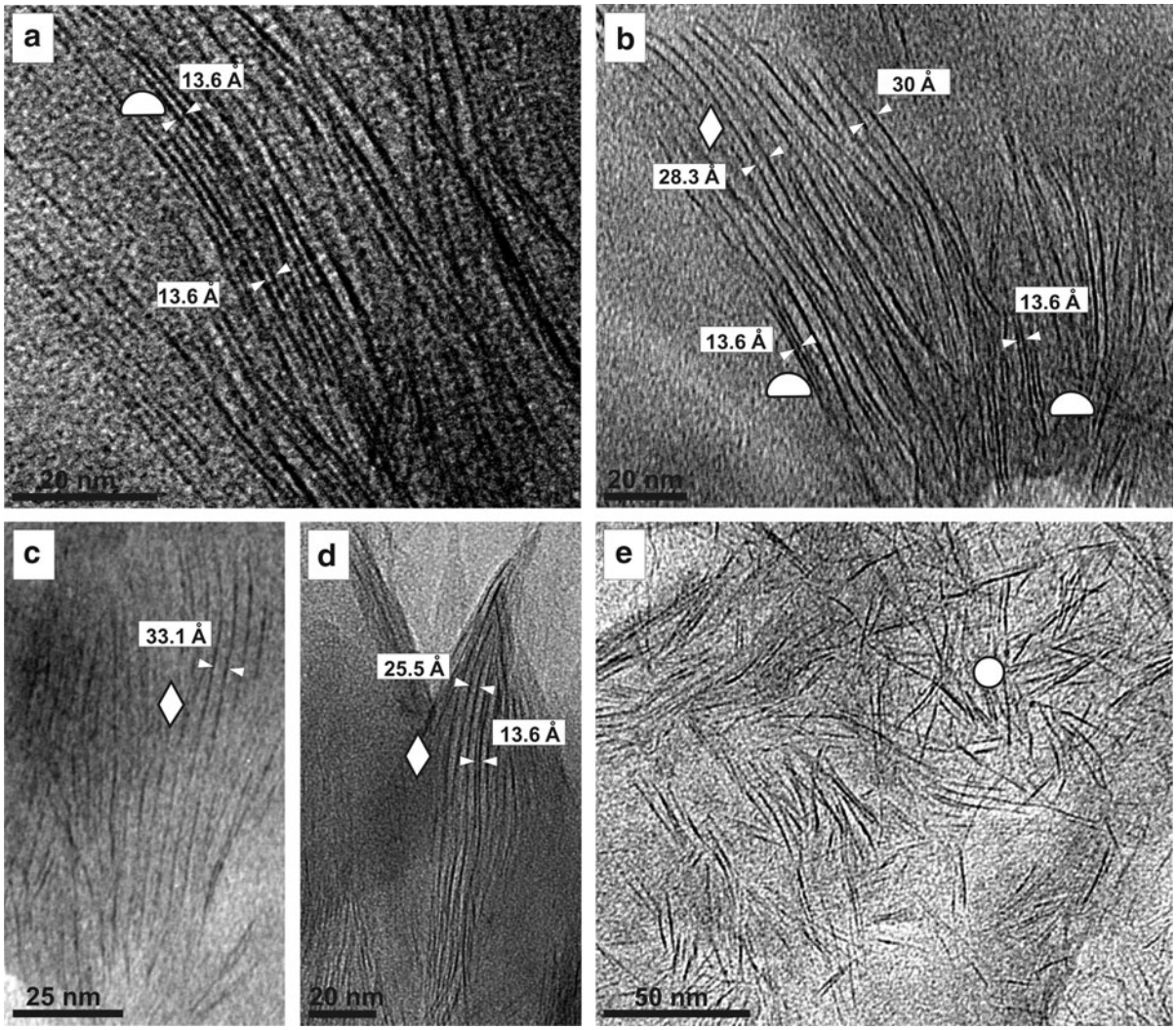

FIG. 4. HRTEM images of the synthesized saponite after treatment with $n_C = 18$ cations showing different types of layer structures: (**a**) short sequences of two to eight 2:1 silicate layers having expanded interlayers of 13.6 Å (white half circles), (**b–d**) sequences of curved to planar 2:1 silicate layers having equally expanded interlayer spacings that range from ~25 to ~33 Å (white diamonds), and (**e**) clusters of disorganized single 2:1 silicate layers (white circle).

predominant highly expanded phase with a spacing ranging between 25 and 33 Å and a less abundant phase with a spacing of 13.6 Å. Lattice-fringe images do not show any 17.67 Å structures. The appearance of highly expanded structures as observed in lattice-fringe images is most likely caused by the additional incorporation of $n_C = 18$ cations owing to the high concentration of the exchange solution and the nature of the washing procedure that does not guarantee the removal of all excess $n_C = 18$ cations.

This conclusion is supported by a study of Lee and Kim (2002), who investigated the effect of different concentrations of hexadecyltrimethylammonium (HDTMA) solutions on the expansion behavior of smectite-group minerals. The X-ray diffractograms of their study show first-order reflections between 27.6 and 40.5 Å for smectite-group minerals treated with a solution of HDTMA that had a concentration equivalent to 1.5–2.5 times the cation exchange capacity of the samples. Additional incorporation of HDTMA in the interlayer space and subsequent higher expansion occurs through hydrophobic bonding if the alkylammonium molecule loading onto the clay-mineral particle increases beyond the cation exchange capacity of the material (their Fig. 10d). A relatively high concentration of a solution of octadecylammonium hydrochloride (40–50%) was also used in the present study, and therefore it is possible that excess $n_C = 18$ cations entered the interlayer space resulting in the high expansion of the saponite crystal packets as suggested by Lee and Kim (2002). After the exchange with $n_C = 18$ cations, the ultrathin sections of this study were gently washed in a Petri dish filled with preheated distilled water, which was clearly insufficient to achieve the complete removal of all excess $n_C = 18$ cations from the interlayer space. Therefore, the crystals with excess $n_C = 18$ cations in the interlayer space appear in lattice-fringe images as highly expanded sequences of 2:1 silicate layers, which is the case for the majority of synthesized saponite crystals. Silicate layers with an expansion between 13 and 14 Å have a monolayer arrangement of the $n_C = 18$ molecules in their interlayer spaces. The interlayer charge density is low, and therefore the *n*-alkylammonium chains have sufficient space to arrange themselves as flat-

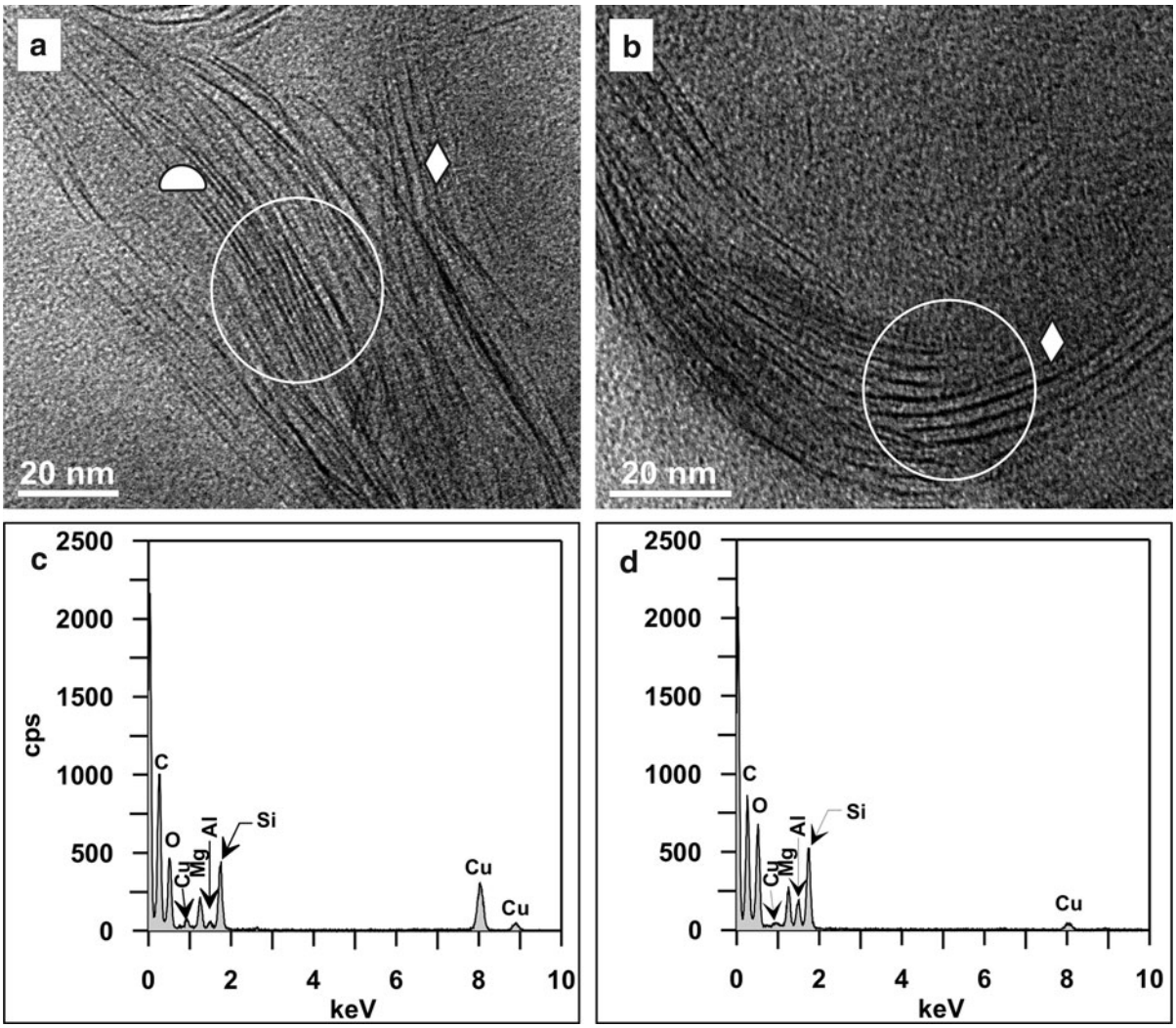

FIG. 5. HRTEM images of differently expanded saponite crystal sequences and corresponding EDS analyses. (**a**) Sequences of 2:1 silicate layers having expanded interlayers of ~13–14 Å (white half circle) and a few sequences of 2:1 silicate layers having expanded interlayers that range from ~25 to ~33 Å (white diamond). (**b**) HRTEM image showing sequences of 2:1 silicate layers with expanded interlayers that range from ~25 to ~33 Å (white diamond). (**c**) EDS analysis of the area marked by a white circle in (a). (**d**) EDS spectrum of the area marked by a white circle in (b). The EDS spectra show that the lattice fringes have the chemical composition of saponite. The lattice fringes contain Si, Mg, and Al. Each lattice fringe (black line) is composed of an octahedral sheet sandwiched between two tetrahedral sheets (T-O-T). The pattern does not show K as it was readily exchanged by the $n_C = 18$ cations. The EDS analyses also showed that the 2:1 layer silicates with the larger interlayer expansion, *i.e.,* higher interlayer charge (white diamond), have more Al in their crystal structure than the less expanded structures (white half circle) (see Al peak in the EDS analyses; Cu peaks are from the TEM grid). The intensity of these peaks depends on the distance between the location of the analysis and the copper bars of the grid. The C peak may originate from the carbon support film on the grid, the $n_C = 18$ cations, and/or from the embedding resin.

lying monolayers. Based upon X-ray diffraction analyses, Maes *et al.* (1979) showed that the transition from a monolayer (13.6 Å) to a bilayer (17.7 Å) arrangement only occurs if the layer charge of the 2:1 layer silicates is >0.24 eq/$O_{10}(OH)_2$. This seems to be the case for most of the synthesized saponite crystals of this study since the XRD pattern of the $n_C = 18$ cation–exchanged material shows a 17.67 Å peak. The transition from the monolayer to bilayer arrangement in samples for XRD analysis was achieved during the 5-day exchange procedure. In contrast, the duration of 20 min used for the "on-grid-exchange-procedure" for ultrathin sections seems to have been too short and the interlayer charge too low to achieve a bilayer arrangement within the interlayer space of the low-charge 2:1 silicate layers (13 to 14 Å) that formed during the synthesis experiment. Therefore, lower-charge smectite crystallites or low-charge layers within an otherwise high-charge smectite 2:1 silicate layer sequence have a 13–14 Å spacing in the lattice-fringe images.

The capability of the smectite-group mineral montmorillonite to provide catalytic assistance for the polymerization and synthesis of amino acids and nucleotides as well as more complex organic molecules like RNA has been extensively demonstrated in the literature (Ertem and Ferris, 1996, 1998, 2000; Ferris, 2002; Franchi and Gallori, 2005). The aspect of

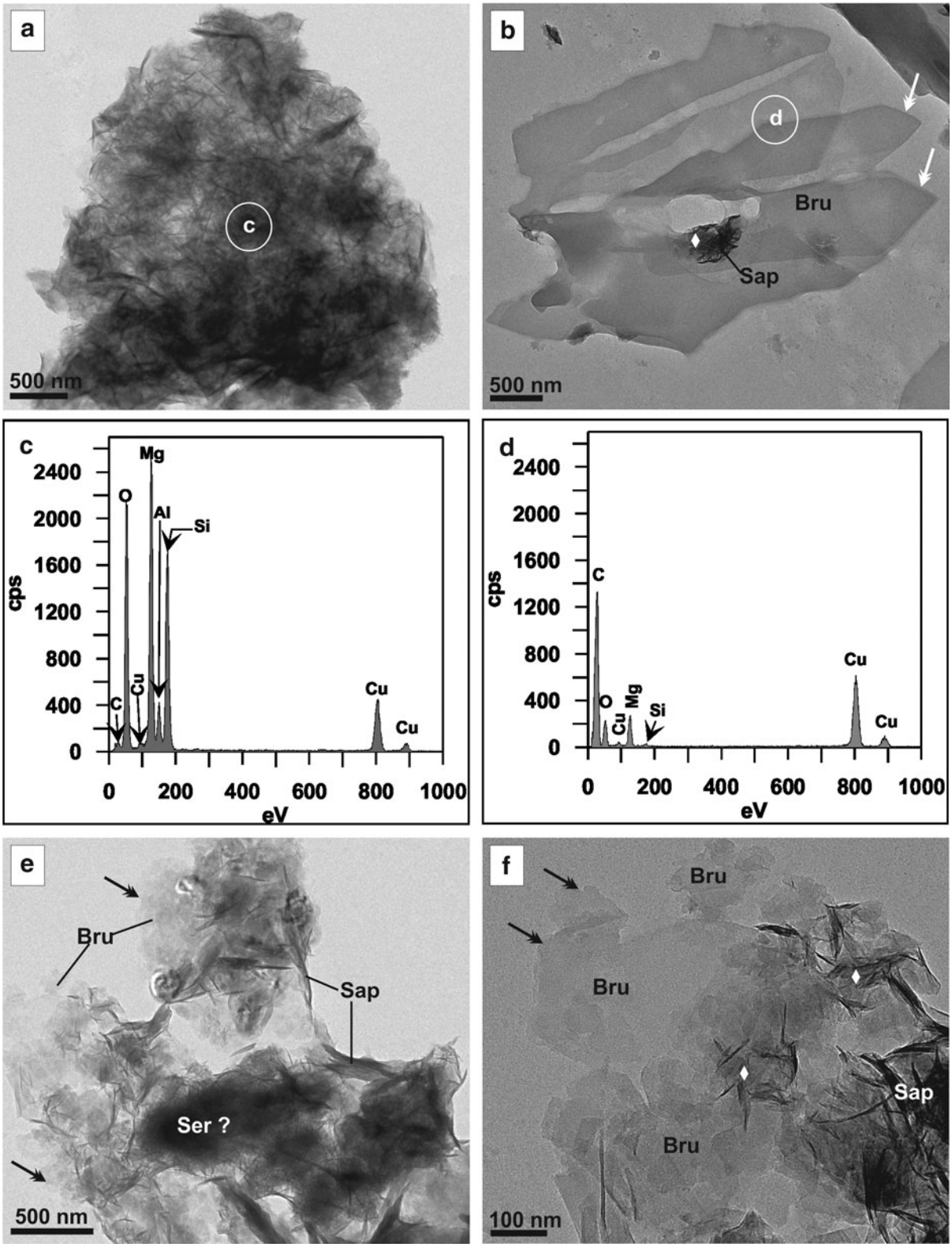

FIG. 6. TEM images of the synthesis products of experiment 2. (**a**) Overview images showing globular aggregates of whisker- and needle-like crystals. (**b**) Tabular brucite crystals (Bru) that developed some well-pronounced crystal faces (white arrows). A small nest of saponite (Sap) seems to originate from within the brucite crystal aggregate (white diamond). (**c**–**d**) EDS analyses of the aggregates shown in (a) and (b). The locations of the analyses are marked with circles in (a) and (b). (**e**) Overview image showing brucite (Bru), saponite (Sap), and possibly a serpentine phase (Ser). (**f**) Overview image showing saponite (Sap) and brucite (Bru). Nucleation sites of saponite crystal packets within the brucite aggregates are indicated by white diamonds.

replicating capabilities of the smectite-group minerals relevant to the origin of prebiotic life has not been addressed. More than 50 years ago, it was proposed that clay minerals and their capacity to concentrate organic molecules on their surfaces might have played an important role in the polymerization of amino acids and the evolution toward the first primitive forms of life (Bernal, 1949). This idea was further promoted by Cairns-Smith (1965), who suggested that layer silicates were like DNA capable of replication by means of a surface template-catalyzed polymerization of the layer silicates composed of Si-tetrahedral and the Al-octahedral sheets.

> According to the specific theory that is proposed, the primitive genographs were patterns of substitutions in colloidal clay crystallites. (The theoretical information density in such a crystallite is comparable to that in DNA.) Evolution proceeded through selective elaboration of substitutional genographs that had survival value for the clay crystallites that held them (at first through genetically controlled adsorption of a "spectrum" of organic molecules) within a complex, dynamic, primitive environment. (Cairns-Smith, 1965)

The clay-mineral crystals grow through the addition of individual Si-O tetrahedra and Al/Mg-O octahedra onto the edges of the tetrahedral and octahedral sheets; hence information contained in the domain structure and chemistry is replicated in these complex layer silicate structures (Cairns-Smith and Hartman, 1986).

This replication mechanism has been documented with kaolinite as a model whereby the nucleation and growth of individual layers takes place through screw dislocations resulting in replicating layers that have the same domain structure, shape, and chemistry. While there is little doubt that kaolinite is an excellent replication system, the drawback with this model is that kaolinite is a poor catalyst, and the screw dislocation accounts for only one process of kaolinite growth. Hartman (1998) suggested that smectite-group minerals rather than kaolinite were better suited to adsorb and concentrate organic molecules on their surfaces. However, the replicating structure of smectite-group minerals has never been demonstrated until now. In this study, the lattice-fringe images of the saponite crystallites after treatment with $n_C = 18$ cations clearly document the replication of possibly different generations of 2:1 silicate layer sequences with distinct chemical and structural composition *within* the same sample.

The existence of differently expanded 2:1 layer silicate structures as shown in the lattice-fringe images suggests the crystallization of T-O-T layers with different levels of Al^{3+} substitution in the tetrahedral sheets resulting in lower or higher negative charges of these layers. These differences in the structural charge distribution of individual 2:1 layer silicates cannot be deciphered by XRD alone, as the diffraction pattern results from the constructive interference of many coherent sequences of 2:1 layer silicates. In contrast, the analysis of lattice-fringe images enables the distinction between individual packets of saponite crystallites with different interlayer charge values and of charge differences even within single 2:1 silicate layers. This is possible because the individual interlayer spacings can be directly measured. The variation of the interlayer spacing is a result of the differences in interlayer charge, which in turn reflects the amount of isomorphous substitutions within the T-O-T layers.

EDS analyses showed the differences in Al concentration between highly expanded and less expanded 2:1 layer silicate structures (Fig. 5). Two possible scenarios could explain the growth of differently charged 2:1 layer silicates in the synthesis experiments of this study. First, the growth of the differently charged 2:1 layer silicates may occur in several generations, and second, the formation of T-O-T nucleation sites with different Si/Al ratios may occur simultaneously. The crystal growth process from the gel involving subsequent generations may have started with the formation of highly expanded structures (25–33 Å with paraffin-like arrangement of $n_C = 18$ cations), which incorporated more Al^{3+} into their silica sheets since Al^{3+} was readily available in the starting gel. After the aluminum concentration decreased, less Al^{3+} was incorporated into the tetrahedral sites, resulting in the formation of saponite crystallites with lower interlayer charges that show an expansion of 13.6 Å after treatment with $n_C = 18$ cations. The highly expanded structures are the dominant phase in synthesis experiment 1 (Figs. 3 and 4). After the Al^{3+} was exhausted, the remaining Si and Mg may have been incorporated into the talc-like phase. The scenario of simultaneous growth of high-charge and low-charge 2:1 layer silicates from the gel would require the formation of T-O-T nucleation sites with different Si^{4+}/Al^{3+} ratios. Once the different T-O-T nucleation sites had formed, the subsequent accretion of new tetrahedra or octahedra extending the tetrahedral and octahedral sheets in the [100] and [010] directions acquired the same element ratios that were inherited from the nucleation site. A simultaneous growth could be supported by the presence of crystals that contain both low-charge and high-charge 2:1 silicate layers (Fig. 4d). Talc could also form concomitantly with the crystallization of saponite if a phase equilibrium exists between the Al-bearing species (saponite) and the Al-depleted species (talc).

The 2:1 layer silicates with uniformly expanded interlayer spaces suggest that the layer charges and charge distributions are similar or equal to consecutive T-O-T layers within one packet (Figs. 3, 4, 5). From this observation, we may conclude that during the growth of a 2:1 layer silicate packet the amount of Al^{3+} substituted for Si^{4+} stays more or less constant from layer to layer. Thus, the pattern of Al substitution occurs in such a way that the interlayer charges are more or less equally distributed, causing such regularly expanded 2:1 layer silicate packets. Independent of whether the highly expanded (higher amount of Al^{3+} substitutions) and less expanded (lower amount of Al^{3+} substitutions) 2:1 layer silicate packets were formed at the same time or as different generations, in both situations the Si/Al ratio seems to be passed on from layer to layer by heritage. This is demonstrated by the regular interlayer expansion within the packets (Figs. 4a–d, 5a, 5b).

5. Conclusions

This study demonstrates how oxalate promotes the crystallization of saponite from a silicate gel at 60°C and ambient pressure. The treatment of the synthesis products with octadecylammonium cations ($n_C = 18$) in combination with HRTEM imaging enables the differentiation between single layers and packets of 2:1 layer silicates that have differently expanded interlayer spaces, which is not possible by XRD

analysis. The difference in interlayer expansion results from the variation in the substitution of Al^{3+} for Si^{4+} within the tetrahedral sheets of the saponite crystallites. The Si/Al ratio seems to be passed on from layer to layer by heritage, which is demonstrated by the regular interlayer expansion within the packets. The experimental conditions of this study might in part and also in a very simplified manner resemble the near-surface temperature conditions on parent planetoid bodies or pressure and temperature conditions on the surface of early Earth. Magnesium- and iron-rich clay minerals are abundant alteration products in carbonaceous chondrites and most likely were also abundant on early Earth due to the alteration of its mafic and ultramafic crust. Organic molecules like oxalate present in lower-temperature hydrothermal fluids that percolated through fracture networks in parent planetoid bodies of carbonaceous chondrites or through the crust of early Earth could have catalyzed the formation of clay-mineral crystals, which in turn formed clay microenvironments that provided abundant adsorption sites for other organic molecules that were present in solution. The interaction among these adsorbed molecules could have led to the polymerization of more complex organic molecules like DNA or RNA from nucleotides.

The template-catalyzed polymerization of clay formation as observed in the saponite packets of the present study could have been a possible amplification mechanism for the enrichment of chiral molecules in carbonaceous chondrite meteorites or even on ancient Earth.

In future experiments, we will synthesize iron-rich saponite under anaerobic conditions and explore experimentally the possible role of these clay minerals in the origin and evolution of prebiotic macromolecules essential to the development of life.

Acknowledgments

C.G. Whitney is gratefully acknowledged for providing the synthetic silica gel, and Jeannie Mui and Lee Ann Monaghan of the Facility for Electron Microscopy Research are thanked for the preparation of ultrathin sections used in the HRTEM analysis. The authors wish to acknowledge the reviewers' constructive recommendations and in-depth reviews, which have greatly improved the quality of the manuscript. This work was supported by grants from the Natural Science and Engineering Research Council of Canada (H.V. and R.H.) and the Fonds Québécois de la Recherche sur la Nature et les Technologies to the Centre for Biorecognition and Biosensors (H.V.).

Author Disclosure Statement

No competing financial interests exist.

Abbreviations

EDS, energy-dispersive spectroscopy; EG, ethylene glycol; HDTMA, hexadecyltrimethylammonium; HRTEM, high-resolution transmission electron microscopy; TEM, transmission electron microscopy; XRD, X-ray diffraction.

References

Anders, E. (1963) On origin of carbonaceous chondrites. *Ann NY Acad Sci* 108:514–533.

Balogh, M. and Laszlo, P. (1993) *Organic Chemistry Using Clays,* Springer-Verlag, Berlin.

Barber, D.J. (1981) Matrix phyllosilicates and associated minerals in C2M carbonaceous chondrites. *Geochim Cosmochim Acta* 45:945–970.

Bass, M.N. (1971) Montmorillonite and serpentine in Orgueil meteorite. *Geochim Cosmochim Acta* 35:139–147.

Becker, R.H. and Epstein, S. (1982) Carbon, hydrogen and nitrogen isotopes in solvent-extractable organic-matter from carbonaceous chondrites. *Geochim Cosmochim Acta* 46:97–103.

Bernal, J.D. (1949) The physical basis of life. *Proceedings of the Physical Society of London Section A* 62:537–558.

Brearley, A.J. (1997) Phyllosilicates in the matrix of the unique carbonaceous chondrite Lewis Cliff 85332 and possible implications for the aqueous alteration of CI chondrites. *Meteorit Planet Sci* 32:377–388.

Brindley, G.W. (1981) Structures and chemical composition of clay minerals. In *Clays and the Resource Geologist: A Short Course,* edited by F.J. Longstaffe, Mineralogical Association of Canada, Québec, pp 1–21.

Bunch, T.E. and Chang, S. (1980) Carbonaceous chondrites. 2. Carbonaceous chondrite phyllosilicates and light-element geochemistry as indicators of parent body processes and surface conditions *Geochim Cosmochim Acta* 44:1543–1577.

Cairns-Smith, A.G. (1965) The origin of life and the nature of the primitive gene. *J Theor Biol* 10:53–88.

Cairns-Smith, A.G. and Hartman, H., editors. (1986) *Clay Minerals and the Origin of Life,* Cambridge University Press, Cambridge.

Chang, S. and Bunch, T.E. (1986) Clays and organic matter in meteorites. In *Clay Minerals and the Origin of Life,* edited by A.G. Cairns-Smith and H. Hartman, Cambridge University Press, Cambridge, pp 116–129.

Cody, G.D., Boctor, N.Z., Brandes, J.A., Filley, T.R., Hazen, R.M., and Yoder, H.S. (2004) Assaying the catalytic potential of transition metal sulfides for abiotic carbon fixation. *Geochim Cosmochim Acta* 68:2185–2196.

Cronin, J.R., Pizzarello, S., Epstein, S., and Krishnamurthy, R.V. (1993) Molecular and isotopic analyses of the hydroxy-acids, dicarboxylic-acids, and hydroxydicarboxylic acids of the Murchison meteorite. *Geochim Cosmochim Acta* 57: 4745–4752.

Delaney, J.R., Kelley, D.S., Lilley, M.D., Butterfield, D.A., Baross, J.A., Wilcock, W.S.D., Embley, R.W., and Summit, M. (1998) The quantum event of oceanic crustal accretion: impacts of diking at mid-ocean ridges. *Science* 281:222–230.

Drits, V.A., Khvorova, I.V., Sokolova, A.L., and Voronin, B.I. (1989) Clay minerals in deep water hydrothermal structures of the Guaymas Depression (Gulf of California). *Lithology and Mineral Resources* 24:10–15.

Ertem, G. and Ferris, J.P. (1996) Synthesis of RNA oligomers on heterogeneous templates. *Nature* 379:238–240.

Ertem, G. and Ferris, J.P. (1998) Formation of RNA oligomers on montmorillonite: site of catalysis. *Orig Life Evol Biosph* 28: 485–499.

Ertem, G. and Ferris, J.P. (2000) Sequence- and regio-selectivity in the montmorillonite-catalyzed synthesis of RNA. *Orig Life Evol Biosph* 30:411–422.

Ferris, J.P. (2002) Montmorillonite catalysis of 30–50 mer oligonucleotides: laboratory demonstration of potential steps in the origin of the RNA world. *Orig Life Evol Biosph* 32:311–332.

Franchi, M. and Gallori, E. (2005) A surface-mediated origin of the RNA world: biogenic activities of clay-adsorbed RNA molecules. *Gene* 346:205–214.

Fraser, D.G., Greenwell, H.C., Skipper, N.T., Smalley, M.V., Wilkinson, M.A., Deme, B., and Heenan, R.K. (2011a) Chiral interactions of histidine in a hydrated vermiculite clay. *Phys Chem Chem Phys* 13:825–830.

Fraser, D.G., Fitz, D., Jakschitz, T., and Rode, B.M. (2011b) Selective adsorption and chiral amplification of amino acids in vermiculite clay—implications for the origin of biochirality. *Phys Chem Chem Phys* 13:831–838.

Geptner, A., Kristmannsdottir, H., Kristjansson, J., and Marteinsson, V. (2002) Biogenic saponite from an active submarine hot spring, Iceland. *Clays Clay Miner* 50:174–185.

Glavin, D.P. and Dworkin, J.P. (2009) Enrichment of the amino acid L-isovaline by aqueous alteration on CI and CM meteorite parent bodies. *Proc Natl Acad Sci USA* 106:5487–5492.

Hamilton, D.L. and Henderson, C.M.B. (1968) The preparation of silicate compositions by a gelling method. *Mineral Mag* 36:832–838.

Hanczyc, M.M., Fujikawa, S.M., and Szostak, J.W. (2003) Experimental models of primitive cellular compartments: encapsulation, growth, and division. *Science* 302:618–622.

Hartman, H. (1998) Photosynthesis and the origin of life. *Orig Life Evol Biosph* 28:515–521.

Hartman, H., Sweeney, M.A., Kropp, M.A., and Lewis, J.S. (1993) Carbonaceous chondrites and the origin of life. *Orig Life Evol Biosph* 23:221–227.

Hem, J.D. and Lind, C.J. (1974) Kaolinite synthesis at 25 degrees C. *Science* 184:1171–1173.

Jones, C.L. and Brearley, A.J. (2006) Experimental aqueous alteration of the Allende meteorite under oxidizing conditions: constraints on asteroidal alteration. *Geochim Cosmochim Acta* 70:1040–1058.

Jones, T.D., Lebofsky, L.A., Lewis, J.S., and Marley, M.S. (1990) The composition and origin of the C, P, and D asteroids—water as a tracer of thermal evolution in the outer belt. *Icarus* 88:172–192.

Koehler, B., Singer, A., and Stoffers, P. (1994) Biogenic nontronite from marine white smoker chimneys. *Clays Clay Miner* 42:689–701.

La Iglesia, A. and Galan, E. (1975) Halloysite-kaolinite transformation at room-temperature. *Clays Clay Miner* 23:109–113.

La Iglesia, A. and Martin Vivaldi, J.L. (1972) A contribution to the synthesis of kaolinite. In *Proceedings of the International Clay Conference,* edited by J.M. Serratosa and A. Sanchez, Division de Ciencias CSIC, Madrid, pp 85–173.

Lagaly, G. (1981) Inorganic layer compounds—phenomena of interface reactions with organic compounds. *Naturwissenschaften* 68:82–88.

Lagaly, G. (1982) Layer charge heterogeneity in vermiculites. *Clays Clay Miner* 30:215–222.

Lagaly, G. and Dékany, I. (2005) Adsorption on hydrophobized surfaces: clusters and self-organization. *Adv Colloid Interface Sci* 114–115:189–204.

Lagaly, G. and Weiss, A. (1969) Determination of layer charge in mica-type layer silicates. In *Proceedings of the International Clay Conference,* Vol. 1, edited by L. Heller, Israel Universities Press, Jerusalem, pp 61–80.

Lagaly, G. and Weiss, A. (1970) Arrangement and orientation of cationic tensides on silicate surfaces. 3. Paraffin-like structures in alkylammonium layer silicates with an average layer load (vermiculite). *Kolloid-Zeitschrift und Zeitschrift für Polymere* 238:485–493.

Lee, S.Y. and Kim, S.J. (2002) Expansion of smectite by hexadecyltrimethylammonium. *Clays Clay Miner* 50:435–445.

Lee, T. (1979) New isotopic clues to solar-system formation. *Rev Geophys* 17:1591–1611.

Linares, J. and Huertas, F. (1971) Kaolinite-synthesis at room temperature. *Science* 171:896–897.

Maes, A., Stul, M.S., and Cremers, A. (1979) Layer charge-cation-exchange capacity relationships in montmorillonite. *Clays Clay Miner* 27:387–392.

Malla, P.B. and Douglas, L.A. (1987) Identification of expanding layer silicates: layer charge vs. expansion properties. In *International Clay Conference,* The Clay Minerals Society, Bloomington, IN, pp 277–283.

Marteinsson, V.T., Birrien, J.L., and Prieur, D. (1997) *In situ* enrichment and isolation of thermophilic microorganisms from deep-sea vent environments. *Can J Microbiol* 43:694–697.

McSween, H.Y., Jr. (1987) Aqueous alteration in carbonaceous chondrites: mass balance constraints on matrix mineralogy. *Geochim Cosmochim Acta* 51:2469–2477.

Meunier, A., Petit, S., Cockell, C.S., El Albani, A., and Beaufort, D. (2010) The Fe-rich clay microsystems in basalt-komatiite lavas: importance of Fe-smectites for pre-biotic molecule catalysis during the Hadean Eon. *Orig Life Evol Biosph* 40, doi:10.1007/s11084-010-9205-2.

Pizzarello, S., Zolensky, M., and Turk, K.A. (2003) Nonracemic isovaline in the Murchison meteorite: chiral distribution and mineral association. *Geochim Cosmochim Acta* 67:1589–1595.

Sears, S.K., Hesse, R., and Vali, H. (1998) Significance of n-alkylammonium exchange in the study of 2:1 clay mineral diagenesis, Mackenzie Delta Beaufort Sea region, Arctic Canada. *Can Mineral* 36:1485–1506.

Shimazu, H. and Terasawa, T. (1995) Electromagnetic induction-heating of meteorite parent bodies by the primordial solar-wind. *J Geophys Res* 100:16923–16930.

Shock, E.L. (1990) Geochemical constraints on the origin of organic compounds in hydrothermal systems. *Orig Life Evol Biosph* 20:331–367.

Siffert, B. (1962) Quelques réactions de la silice en solution: la formation des argiles. In *Mémoires du Service de la Carte Géologique d'Alsace et de Lorraine,* Issue 21, Service de la Carte Geologique d'Alsace et de Lorraine, Strasbourg, France.

Siffert, B. (1986) The role of organic complexing agents. In *Clay Minerals and the Origin of Life,* edited by A.G. Cairns-Smith and H. Hartman, Cambridge University Press, Cambridge, pp 75–78.

Small, J.S. and Manning, D.A.C. (1993) Laboratory reproduction of morphological variation in petroleum reservoir clays: monitoring of fluid composition during illite precipitation. In *Geochemistry of Clay Pore Fluid Interactions,* edited by D.A.C. Manning, P.L. Hall, and C.R. Hughess, Mineralogical Society/Chapman and Hall, London, pp 181–212.

Small, J.S., Hamilton, D.L., and Habesch, S. (1992) Experimental simulations of clay precipitation within reservoir sandstones. 2. Mechanism of illite formation and controls on morphology. *J Sediment Petrol* 62:520–529.

Tomeoka, K. and Ohnishi, I. (2010) Indicators of parent-body processes: hydrated chondrules and fine-grained rims in the Mokoia CV3 carbonaceous chondrite. *Geochim Cosmochim Acta* 74:4438–4453.

Vali, H. and Hesse, R. (1990) Alkylammonium treatment of clay minerals in ultrathin sections—a new method for HRTEM examination of expandable layers. *Am Mineral* 75:1443–1446.

Vali, H. and Hesse, R. (1992) Identification of vermiculite by transmission electron microscopy and X-ray diffraction. *Clay Minerals* 27:185–192.

Vali, H., Hesse, R., and Kohler, E.E. (1991) Combined freeze-etch replicas and HRTEM images as tools to study fundamental particles and the multiphase nature of 2:1 layer silicates. *Am Mineral* 76:1973–1984.

Vali, H., Hesse, R., and Martin, R.F. (1994) A TEM-based definition of 2:1 layer silicates and their interstratified constituents. *Am Mineral* 79:644–653.

Velde, B. and Meunier, A. (2008) *The Origin of Clay Minerals in Soils and Weathered Rocks,* Springer-Verlag, Berlin.

Whitney, G. (1983) Hydrothermal reactivity of saponite. *Clays Clay Miner* 31:1–8.

Zahnle, K., Arndt, N., Cockell, C.S., Halliday, A., Nisbet, E., Selsis, F., and Sleep, N.H. (2007) Emergence of a habitable planet. *Space Sci Rev* 129:35–78.

Address correspondence to:
Hojatollah Vali
Facility for Electron Microscopy Research
McGill University
3640 University Street
Montréal, QC
H3A 0C7
Canada

E-mail: hojatollah.vali@mcgill.ca

Submitted 24 February 2011
Accepted 1 April 2012